

Isotopic signature of core-derived SiO₂

George Helffrich^{1,*}, Anat Shahar², Kei Hirose^{1,3}

ms. for resubmission to *American Mineralogist*: first rev. 7 Feb. 2018;
submitted 26 Jan. 2018; original submitted 28 Nov. 2017

¹Earth-Life Science Institute, Tokyo Institute of Technology, 2-12-1 Ookayama 17E-312, Meguro-ku, Tokyo 152-8550, Japan

²Geophysical Laboratory, Carnegie Institution for Science, 5251 Broad Branch Road NW, Washington DC 20015, USA

³Earth and Planetary Sciences Dept., University of Tokyo, 7-3-1 Hongo, Bunkyo-ku, Tokyo 113-0033 Japan

ABSTRACT

We apply an experimentally based thermodynamic model of Si+O saturation for the core to determine the saturation level of these elements under the conditions when the core formed. The model limits the bulk Si content of the core to between 0.4 and 3.1 wt% depending on the pressure, temperature and oxygen content of the metal when it segregated from silicate. With knowledge of the core's Si content, the measured ³⁰Si content of the silicate Earth, and the experimentally determined metal-silicate fractionation factor, we can calculate the core's $\delta^{30}\text{Si}$, which is between -0.92 to -1.36 ‰. SiO₂ cycled through the core and then released into the mantle might be trapped in inclusions in diamond formed in the lower mantle. These would be characterized by significantly lighter $\delta^{30}\text{Si}$ values of -1.12 ± 0.13 (1 σ) ‰, compared to bulk silicate earth values of -0.29 ‰ and a potentially key indicator of mass transfer from the core to the mantle.

INTRODUCTION

The Earth formed through a relatively rapid process during which approximately chondritic materials aggregated as a discrete body from the protoplanetary disk and

*E-mail: george@elsi.jp

25 differentiated into a metallic core and a silicate crust and mantle (Wood et al., 2006).
26 During the melting arising from the accretion process (from impact energy, heat produc-
27 tion from short-lived radionuclides, gravitational potential energy release from differenti-
28 ation), either a planetary-scale magma ocean or spatially restricted magma lakes arose,
29 imparting a relatively low pressure differentiation signal (compared to the pressures of ei-
30 ther the core-mantle boundary (CMB) or the planet's center) on the moderately
31 siderophile elements (Li and Agee, 1996; Wade and Wood, 2005; Siebert et al., 2011;
32 2013; Fischer et al., 2015).

33 Concurrent with siderophile element partitioning, some major elements also entered
34 the metal destined for the core: Si, O, and Mg are potential candidates (O'Neill et al.,
35 1998; O'Rourke and Stevenson, 2016; Badro et al., 2016; Hirose et al., 2017). In particu-
36 lar, some Si is believed to reside in the core because the Mg/Si and Al/Si ratios in the
37 bulk silicate Earth are higher than chondritic values (Palme and O'Neill, 2003). Based on
38 high-pressure experiments at CMB conditions, Hirose et al. (2017) developed a model for
39 SiO₂ saturation in core metal that allows the amount of Si+O potentially ingested by the
40 core during accretion to be assessed. The Si+O is subsequently expelled back into the
41 mantle as SiO₂ as the core cools. Escape of SiO₂ from the core is virtually certain due to
42 its low density relative to silicate at the CMB (Hirose et al., 2017). This cycling through
43 the core imprints core-derived Si with the metal-silicate stable isotope fractionation pre-
44 vailing at the conditions of differentiation (Georg et al., 2007; Shahar et al., 2011) rather
45 than bulk silicate Earth values and potentially provides a way to identify SiO₂ previously
46 hosted by the core. The core's estimated Si content is based on a new, experimentally-

47 based set of constraints not previously exploited, to our knowledge, for making a metal-
48 silicate isotope balance. We explore core-hosted SiO₂ isotopic signatures here; the physi-
49 cal mechanism for expelling SiO₂ from the core is described separately (Helffrich et al.,
50 2018).

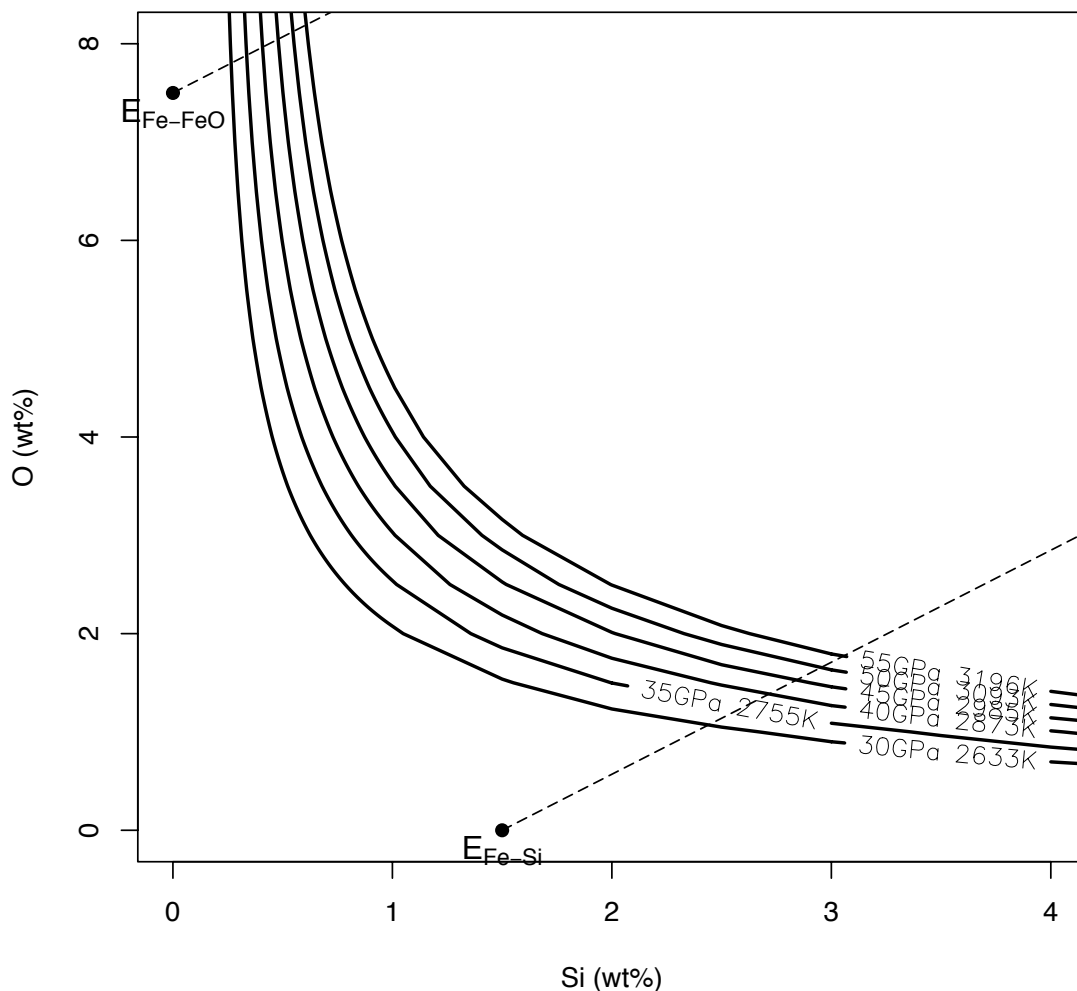
51

METHODS

52 We use Hirose et al.'s (2017) Si+O solubility model to determine joint Si+O solubility at
53 various pressure (P) and temperature (T) conditions during the course of core formation
54 and cooling. The conditions of core formation are set using a single-stage core formation
55 model to approximate the range of pressures and temperatures encountered during accre-
56 tion. The conditions are set as fractions of the CMB pressure, leading to a P range of
57 30-55 GPa (see Rubie et al. (2011) for one reckoning of the range). From P , the associ-
58 ated T is obtained from two different equations for the peridotite liquidus and solidus,
59 $T(P)$ (Wade and Wood, 2005; Fiquet et al., 2010), respectively. Figure 1 shows a suite of
60 saturation curves at various core formation pressures, calculated by evaluating the joint
61 Si-O saturation expressions at the P and corresponding T on a grid and contouring (Hi-
62 rose et al., 2017).

63 The method we use to estimate Earth's core's Si content is new, and based on joint
64 Si+O solubilities in core metal, the constitution of the Earth's core, and the high-pressure
65 behavior of the eutectic compositions of Fe-Si and Fe-FeO. In particular, Hirose et al.
66 (2017) note that the Earth's inner core requires that it crystallize essentially pure Fe,
67 which restricts the core liquid composition to the intersection of the SiO₂ saturation con-
68 tour and the compositional triangle bounded by SiO₂, the Fe-Si eutectic, and the Fe-FeO

69



70 Figure 1. Saturation of Si and O in metallic iron at a range of pressures corresponding to
71 core formation. Labels on each saturation line are P and T of formation; $T(P)$ from Fi-
72 quet et al. (2010). The Si uptake depends on the O content, and hence yields a range for
73 the mass of Si carried to the core in metal. Quasi-diagonal lines show the SiO_2 loss
74 trend; for inner core properties like Earth's, feasible Si+O contents must be more O-rich
75 than the Fe-Si eutectic (lower line) and less O-rich than the Fe-FeO eutectic (upper line).
76 This limits core Si content to be 0.4-3.1 wt%.

77 eutectic (Fig. 1). The Fe-FeO eutectic moves to higher O content with increasing pres-
78 sure (Komabayashi, 2014; Morard et al., 2017), but the asymptotic behavior of the SiO_2

79 solubility contours with increasing O do not strongly affect the lower bound for Si. In
80 contrast, Fe-Si's eutectic moves Fe-ward at high pressure (Fischer et al., 2013; Ozawa et
81 al., 2016). At the pressure of the Earth's CMB, Fischer et al. (2013) placed the eutectic at
82 5-12 wt% Si, and various estimates of the maximum core Si content by Hin et al. (2014)
83 and Dauphas et al. (2015) placed it at 6-8 and 0-9 wt%, respectively. However, the study
84 by Ozawa et al. (2016) of the eutectic dependence on pressure narrowed the bound con-
85 siderably to ≤ 1.5 wt%, which we use to define the Fe-Si eutectic in the O-free system.
86 Figure 1 depicts the bounds constraining core Si.

87 A Si isotope balance of the Earth (subscript *BE*) may be written in terms of its parti-
88 tioning between the core's metal (subscript *c*) and the mantle and lithosphere's silicate
89 (subscript *BSE*)

$$90 \quad \delta^{30}\text{Si}_{BE} = f_c \delta^{30}\text{Si}_c + (1 - f_c) \delta^{30}\text{Si}_{BSE} \quad . \quad (1)$$

91 f_c is the mass fraction of Si in the core to the Si in the entire Earth. We use a pyrolytic
92 model for the silicate Earth (McDonough and Sun, 1995) to obtain its Si content (21
93 wt%) and the Si+O solubility model to determine the core Si content. To account for the
94 silicate-metal partitioning during core formation, we use Shahar et al.'s (2011) tempera-
95 ture dependent fractionation factor $\Delta^{30}\text{Si}(T) = -7.45(\pm 0.41) \times 10^6/T^2$. Hence,

$$96 \quad \delta^{30}\text{Si}_c = \Delta^{30}\text{Si}(T) + \delta^{30}\text{Si}_{BSE} \quad . \quad (2)$$

97 $\delta^{30}\text{Si}_{BSE}$ is -0.29 ± 0.02 ‰ (Fitoussi et al., 2009), and the *P-T* conditions of core forma-
98 tion sets the fractionation factor and f_c from the Si+O saturation model. From (1) and (2)
99 and these values, $\delta^{30}\text{Si}_{BE}$ may be calculated.

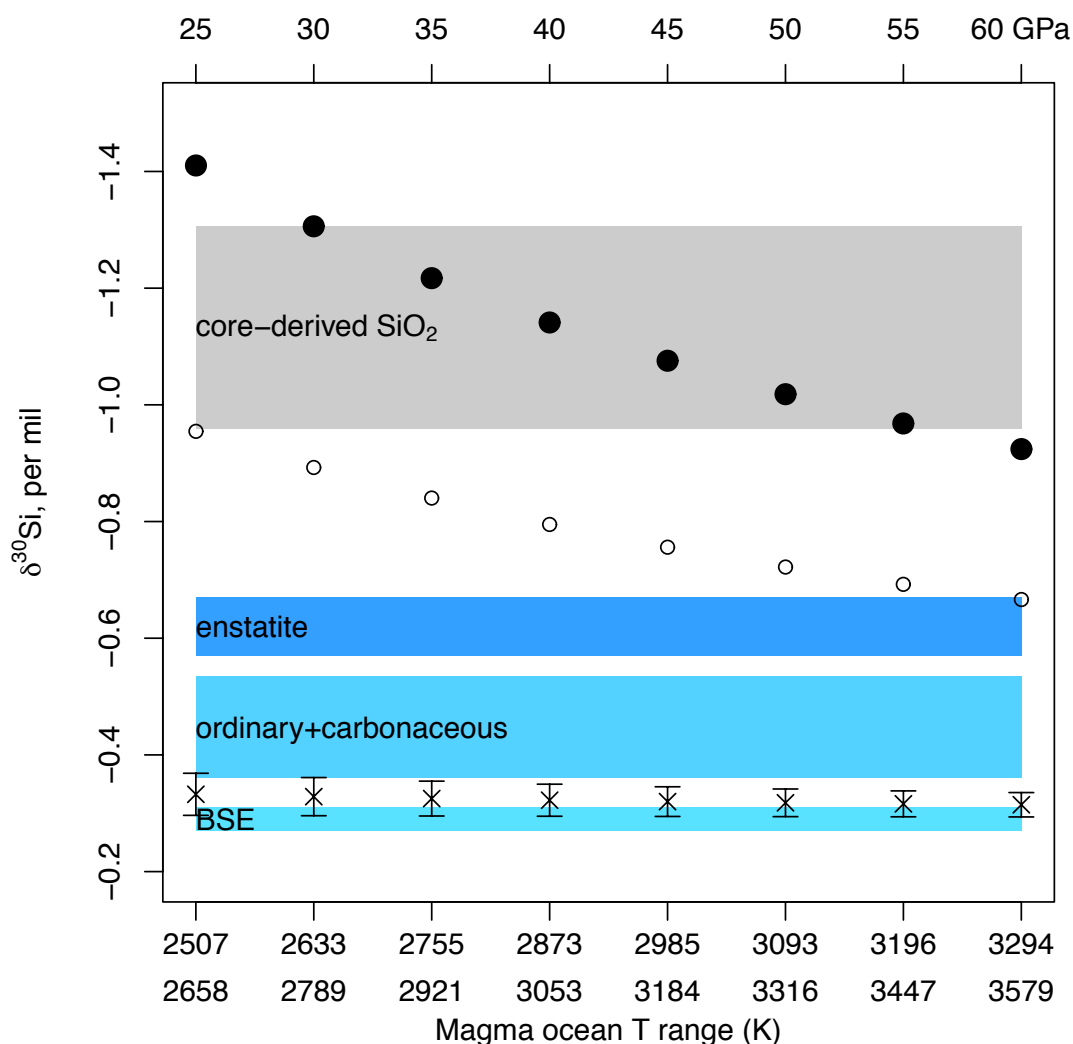
100 We use a single-stage core formation model, but more elaborate methods that track
101 the evolution of the mantle's ^{30}Si content through the accretion process are also possible
102 (Zambardi et al., 2013; Hin et al., 2014). We know experimentally that Si partitioning be-
103 tween metal and silicate is not pressure dependent (Fischer et al., 2015; Hirose et al.,
104 2017) so the core's Si content is fairly constant during accretion (Tuff et al., 2011), yield-
105 ing little difference between multi-stage core formation models and single-stage. Hin et
106 al. (2014) showed that the difference between $\delta^{30}\text{Si}_{BE}$ and $\delta^{30}\text{Si}_{BSE}$ during their accretion
107 histories is never more than 0.3 ‰. The signal that we predict is 3-4 times larger than
108 this, justifying, post-hoc, the use of the single-stage model for obtaining $\delta^{30}\text{Si}_c$.

109 Xu et al. (2017) investigated Si diffusion in stishovite and provided an expression
110 for the pressure- and temperature-dependent Si diffusion coefficient. Using lower mantle
111 pressure and temperature range of 20 GPa, 2000 K - 135 GPa, 4000K (see, e.g. Helffrich
112 (2017)), leads to Si diffusion times over 1 mm distances of at least 300 Myr to 620 Gyr
113 (due, in part, to the diffusion coefficient's strong pressure dependence). Assuming that
114 CaCl_2 -structure SiO_2 , the SiO_2 polymorph stable at higher pressures than stishovite, be-
115 haves similarly, Si isotopic disequilibrium may be maintained over the times required for
116 detection in diamond inclusions.

117 RESULTS

118 Limits on the uptake of Si by the core may be obtained from Figure 1. The present prop-
119 erties of the Earth's core (Hirose et al., 2017), the shape of the saturation contours, and
120 the positions of the Fe-FeO eutectic ($E_{\text{Fe-FeO}}$) and the Fe-Si eutectic ($E_{\text{Fe-Si}}$) control the
121 core's Si content. While the asymptotic nature of the relation at low Si renders the

122



123 Figure 2. Bulk Earth (x) and core-hosted SiO₂ (•,○) ³⁰Si fractionation calculated using
 124 Si+O saturation at various temperatures corresponding to core formation compared to
 125 chondrites. Error bars on each $\delta^{30}\text{Si}_{BE}$ point correspond to variation due to metal-silicate
 126 separation temperature (at pressure given on top scale), O composition of core, and alter-
 127 native $\Delta^{30}\text{Si}(T)$ coefficients. Colored bands show reported range of $\delta^{30}\text{Si}$ of various
 128 chondrite classes (Armytage et al., 2011; Fitoussi et al., 2009; Fitoussi and Bourdon,
 129 2012). Within the uncertainty of the formation conditions, $\delta^{30}\text{Si}_{BE}$ is similar to BSE.
 130 Core-hosted SiO₂ calculated using different fractionation factors (• - Shahar et al. (2011);
 131 ○ - Hin et al. (2014); grey band is $\pm 1\sigma$ of • points) is under most conditions lighter than
 132 chondritic meteorites and BSE, making it a useful diagnostic of core-mantle mass trans-
 133 fer.

134 estimate insensitive to $E_{\text{Fe-FeO}}$, $E_{\text{Fe-Si}}$ and the slope of the SiO_2 loss line define the upper
135 limit of Si saturation. The intersection of the SiO_2 loss line with the saturation contours
136 therefore provides the 3.1 wt% upper bound that we use. These limits set core Si content
137 to be 0.4-3.1 wt%. In turn, the limits place f_c in the range $0.91\% \leq f_c \leq 6.62\%$. By
138 equation (1), the core mass fractions lead to a $\delta^{30}\text{Si}$ fractionation range of
139 $-0.37 \leq \delta^{30}\text{Si}_{BE} \leq -0.30 \text{ ‰}$. Alternative coefficients for $\Delta^{30}\text{Si}(T)$ (Hin et al., 2014;
140 Ziegler et al., 2010) lead to $-0.33 \leq \delta^{30}\text{Si}_{BE} \leq -0.29 \text{ ‰}$. When compared with the val-
141 ues for bulk silicate Earth -0.29 ± 0.02 , we find that the ranges largely overlap. This has
142 implications for the Earth's source materials and formation conditions (Zambardi et al.,
143 2013; Hin et al., 2014; Dauphas et al., 2015), but we do not discuss them here.

144

DISCUSSION

145 Figure 2 shows the ^{30}Si fractionation predicted by the Si+O saturation model. The uncer-
146 tainties include the effective pressure of segregation, alternative temperatures of segrega-
147 tion, and the range of permissible O content of the core, which also affects Si saturation.
148 It is assumed in these calculations that there is no pressure dependent silicon isotope frac-
149 tionation (Shahar et al., 2016) at the temperatures associated with core formation.

150 Depending on the pressure and the solidus temperature model chosen, the Si isotope
151 composition of the core is $-1.12 \pm 0.13 \text{ ‰}$ (1σ), significantly different from the BSE value
152 of $-0.29 \pm 0.02 \text{ ‰}$ (2σ) and all of the chondritic meteorite classes (Figure 2), except at the
153 highest differentiation pressure using the Hin et al. (2014) coefficient. Diamonds are
154 known to trap SiO_2 , including those thought to come from the lower mantle (Stachel et
155 al., 2000; Kaminsky, 2012). Some SiO_2 inclusions are likely to be due to deep

156 subduction of eclogite (Walter et al., 2011) and would have values close to bulk silicate
157 Earth. The signature of a core source for SiO_2 would be an absence of aluminous phases
158 and a light $\delta^{30}\text{Si}$ content of the SiO_2 .

159 The values we report here represent lower bounds on the anticipated $\delta^{30}\text{Si}$ of core-
160 hosted SiO_2 because we are also neglecting any fractionation of ^{30}Si during SiO_2 crystal-
161 lization in the core itself, which will shift $\delta^{30}\text{Si}$ to less negative values. At the end of ac-
162 cretion, the core is likely to be hotter than the mantle and will cool rapidly (Lebrun et al.,
163 2013). The SiO_2 crystallization required to run the Earth's dynamo corresponds to a
164 cooling rate of 50-100 K/Gyr (Hirose et al., 2017), which is significantly lower than
165 ~ 1000 K/Gyr rates expected in early Earth conditions. Hence the bulk of SiO_2 crystal-
166 lized from the core will have separated under correspondingly higher temperatures than
167 that of the present-day CMB. Independent of the $\Delta^{30}\text{Si}(T)$ metal-silicate fractionation
168 factor used, the shift will be within the 1σ uncertainty depicted in Figure 2 if crystalliza-
169 tion initially occurred at 7000-8000 K. Firmer predictions of uncertainty from this source
170 require more detailed models of early Earth evolution focused on the end-stages of accre-
171 tion and evolution past the magma ocean era.

172

IMPLICATIONS

173 The Si+O saturation model developed by Hirose et al. (2017) provides a way to estimate
174 the core's bulk Si content, and to estimate the core and bulk earth ^{30}Si fractionation. We
175 find that the core's $\delta^{30}\text{Si}$ is between -0.92 and -1.36 ‰, depending on the conditions of
176 core formation. The bulk Earth $\delta^{30}\text{Si}$ is $-0.37 \leq \delta^{30}\text{Si}_{BE} \leq -0.30$ ‰, which overlaps
177 bulk silicate Earth and is marginally heavier than the ordinary and carbonaceous

178 chondrite groups. We also predict that any SiO₂ that originated in the core and was later
179 trapped as an inclusion in diamond should have significantly lighter $\delta^{30}\text{Si}$ of around -1.12
180 ± 0.13 ‰.

181 We also described a way to calculate the core's Si content using joint solubility con-
182 straints for Si and O in metal that may prove useful to draw up budgets for other stable
183 isotope systems.

184 ACKNOWLEDGEMENTS

185 Funding partly provided by MEXT/JSPS KAKENHI Grant numbers 15H05832 and 16H06285. Figures
186 and calculations made using R (R Core Team, 2017).

187 REFERENCES

- 188 Armytage, R. M. G., Georg, R. B., Savage, P. S., Williams, H. M. and Halliday, A. N.
189 (2011) Silicon isotopes in meteorites and planetary core formation. *Geochimica et*
190 *Cosmochimica Acta*, 75, 3662–3676.
- 191 Badro, J., Siebert, J. and Nimmo, F. (2016) An early geodynamo driven by exsolution of
192 mantle components from Earth's core. *Nature*, 536, 326–328.
- 193 Dauphas, N., Potraitsson, F., Burkhardt, C., Kobayashi, H. and Kurosawa, K. (2015) Plan-
194 etary and meteoritic Mg/Si and $\delta^{30}\text{Si}$ variations inherited from solar nebula chemistry.
195 *Earth and Planetary Science Letters*, 427, 236–248.
- 196 Fiquet, G., Auzende, A. L., Siebert, J., Corgne, A., Bureau, H., Ozawa, H. and Garbarino,
197 G. (2010) Melting of peridotite to 140 Gigapascals. *Science*, 329, 1516–1518.
- 198 Fischer, R. A., Campbell, A. J., Reaman, D. M., Miller, N. A., Heinz, D. L., Dera, P. and
199 Prakapenka, V. B. (2013) Phase relations in the Fe-FeSi system at high pressures and

- 200 temperatures. *Earth and Planetary Science Letters*, 373, 54–64.
- 201 Fischer, R. A., Nakajima, Y., Campbell, A. J., Frost, D. J., Harries, D., Langenhorst, F.,
202 Miyajima, N., Pollok, K. and Rubie, D. C. (2015) High pressure metal-silicate parti-
203 tioning of Ni, Co, V, Cr, Si, and O. *Geochimica et Cosmochimica Acta*, 167, 177–194.
- 204 Fitoussi, C., Bourdon, B., Kleine, T., Oberli, F. and Reynolds, B. C. (2009) Si isotope
205 systematics of meteorites and terrestrial peridotites: implications for Mg/Si fractiona-
206 tion in the solar nebula and for Si in the Earth’s core. *Earth and Planetary Science Let-*
207 *ters*, 287, 77–85.
- 208 Fitoussi, C. and Bourdon, B. (2012) Silicon isotope evidence against an enstatite chon-
209 drite Earth. *Science*, 335, 1477–1480.
- 210 Georg, R. B., Halliday, A. N., Schauble, E. A. and Reynolds, B. C. (2007) Silicon in the
211 Earth’s core. *Nature*, 447, 1102–1106.
- 212 Helffrich, G., Ballmer, M. D. and Hirose, K. (2018) Core-exsolved SiO₂ dispersal in the
213 Earth’s mantle. *Journal of Geophysical Research*, 122, doi:10.1002/2017JB014865.
- 214 Helffrich, G. (2017) A finite strain approach to thermal expansivity’s pressure depen-
215 dence. *American Mineralogist*, 102, 1690–1695.
- 216 Hin, R. C., Fitoussi, C., Schmidt, M. W. and Bourdon, B. (2014) Experimental determina-
217 tion of the Si isotope fractionation factor between liquid metal and liquid silicate.
218 *Earth and Planetary Science Letters*, 387, 55–66.
- 219 Hirose, K., Morard, G., Sinmyo, R., Umemoto, K., Hernlund, J., Helffrich, G. and
220 Labrosse, S. (2017) Crystallization of silicon dioxide and compositional evolution of
221 the Earth’s core. *Nature*, 543, 99–102.

- 222 Kaminsky, F. (2012) Mineralogy of the lower mantle: A review of ‘super-deep’ mineral
223 inclusions in diamond. *Earth-Science Rev.*, 110, 127–147.
- 224 Komabayashi, T. (2014) Thermodynamics of melting relations in the system Fe-FeO at
225 high pressure: Implications for oxygen in the Earth’s core. *Journal of Geophysical Re-*
226 *search*, 119, 4164–4177.
- 227 Lebrun, T., Massol, H., Chassfière, E., Davaille, A., Marcq, E., Sarda, P., Leblanc, F. and
228 Brandeis, G. (2013) Thermal evolution of an early magma ocean in interaction with the
229 atmosphere. *JGR-Planets*, 118, 1155–1176.
- 230 Li, J. and Agee, C. B. (1996) Geochemistry of mantle-core differentiation at high pres-
231 sure. *Nature*, 381, 686–689.
- 232 McDonough, W. F. and Sun, S.-s. (1995) The composition of the Earth. *Chem. Geol.*,
233 120, 223–253.
- 234 Morard, G., Andrault, G., Antonangeli, D., Nakajima, Y., Auzende, A. L., Boulard, E.,
235 Cervera, S., Clark, A., Lord, O. T., Siebert, J., Svitlyk, V., Garbarino, G. and Mezouar,
236 M (2017) Fe-FeO and Fe-Fe₃C melting relations at Earth’s core-mantle boundary con-
237 ditions: Implications for a volatile-rich or oxygen-rich core. *Earth and Planetary Sci-*
238 *ence Letters*, 473, 94–103.
- 239 O’Neill, H. St.C., Canil, D. and Rubie, D. C. (1998) Oxide-metal equilibria to 2500°C
240 and 25 GPa: Implications for core formation and the light component in the Earth’s
241 core. *Journal of Geophysical Research*, 103, 12,239–12,260.
- 242 O’Rourke, J. G. and Stevenson, D. J. (2016) Powering Earth’s dynamo with magnesium
243 precipitation from the core. *Nature*, 529, 387–389.

- 244 Ozawa, H., Hirose, K., Yonemitsu, K. and Ohishi, Y. (2016) High-pressure melting exper-
245 iments on Fe-Si alloys and implications for silicon as a light element in the core. *Earth*
246 *and Planetary Science Letters*, 456, 47–54.
- 247 Palme H. and C., O’Neil H. S. (2003) Cosmochemical estimates of mantle composition.
248 In H. D. Holland, and K. K. Turekian, Eds., *Treatise on Geochemistry*, 2.
- 249 R Core Team (2017) R: A language and environment for statistical computing, , R Foun-
250 dation for Statistical Computing (<https://www.R-project.org/>), Vienna, Austria.
- 251 Rubie, D. C., Frost, D. J., Mann, U., Asahara, Y., Nimmo, F., Tsuno, K., Kegler, P.,
252 Holzheid, A. and Palme, P. (2011) Heterogeneous accretion, composition and core-
253 mantle differentiation of the Earth. *Earth and Planetary Science Letters*, 301, 31–42.
- 254 Shahar, A., Hillgren, V. J., Young, E. D., Fei, Y., Macris, C. A. and Deng, L. (2011) High-
255 temperature Si isotope fractionation between iron metal and silicate. *Geochimica et*
256 *Cosmochimica Acta*, 75, 7688–2697.
- 257 Shahar, A., Schauble, E. A., Caracas, R., Gleason, A. E., Reagan, M. M., Xiao, Y., Shu, J.
258 and Mao, W. (2016) Pressure-dependent isotopic composition of iron alloys. *Science*,
259 352, 580–582.
- 260 Siebert, J., Badro, J., Antonangeli, D. and Ryerson, F. J. (2013) Terrestrial Accretion Un-
261 der Oxidizing Conditions. *Science*, 339, 1194–1197.
- 262 Siebert, J., Corgne, A. and Ryerson, F. J. (2011) Systematics of metal-silicate partitioning
263 for many siderophile elements applied to Earth’s core formation. *Geochimica et Cos-*
264 *mochimica Acta*, 75, 1451–1489.
- 265 Stachel, T., Harris, J. W., Brey, G. P. and Joswig, W. (2000) Kankan diamonds (Guinea)

- 266 II: Lower mantle inclusion parageneses. *Contributions to Mineralogy and Petrology*,
267 140, 16–27.
- 268 Tuff, J., Wood, B. J. and Wade, J. (2011) The effect of Si on metal-silicate partitioning of
269 siderophile elements and implications for the conditions of core formation. *Geochimica et Cosmochimica Acta*, 75, 673–690.
- 271 Wade, J. and Wood, B. J. (2005) Core formation and the oxidation state of the Earth.
272 *Earth and Planetary Science Letters*, 236, 78–95.
- 273 Walter, M. J., Kohn, S. C., Araujo, D., Bulanova, G. P., Smith, C. B., Gaillou, E., Wang,
274 J., Steele, A. and Shirey, S. B. (2011) Deep mantle cycling of oceanic crust: Evidence
275 from diamonds and their mineral inclusions. *Science*, 334, 54–57.
- 276 Wood, B. J., Walter, M. J. and Wade, J. (2006) Accretion and segregation of its core. *Nature*,
277 441, 825–833.
- 278 Xu, F., Yamazaki, D., Sakamoto, N., Sun, W., Fei, H. and Yurimoto, H. (2017) Silicon
279 and oxygen self-diffusion in stishovite: Implications for stability of SiO₂-rich seismic
280 reflectors in the mid-mantle. *Earth and Planetary Science Letters*, 459, 332–330.
- 281 Zambardi, T., Poitrasson, F., Corgne, A., Méhut, M., Quitté, G. and Anand, M. (2013)
282 Silicon isotope variations in the inner solar system: Implications for planetary forma-
283 tion, differentiation and composition. *Geochimica et Cosmochimica Acta*, 121, 67–83.
- 284 Ziegler, K., Young, E. D., Schauble, E. A. and Wasson, J. T. (2011) Metal-silicate silicon
285 isotope fractionation in enstatite meteorites and constraints on Earth's core formation.
286 *Earth and Planetary Science Letters*, 295, 487–496.